Fermi National Accelerator Laboratory

FERMILAB-Pub-84/107-T
CERN-TH-4015
October, 1984

Vector Boson Production at Present and Future Colliders

G. Altarelli
CERN, Geneva, Switzerland
Dipartimento di Fisica, Univ. di Roma "La Sapienza" †
and INFN, Sezione di Roma, Italy.

R. K. Ellis
Fermi National Accelerator Laboratory
P.O. Box 500, Batavia, IL 60510, USA.

G. Martinelli
INFN, Laboratori Nazionali di Frascati, Italy.

ABSTRACT

We develop in detail the phenomenological implications of our previous analysis of Drell-Yan processes and of vector boson production. Production cross-sections and y, q_T distributions of W and Z^0 in the energy range up to $\sqrt{S}$ = (10-20) TeV are discussed. The problem of W and Z^0 production at super colliders is complicated by the very small values of $\sqrt{\tau} = Q/\sqrt{S}$ involved where $Q = M_{W,Z}$. The novel theoretical features of Drell-Yan processes at very small $\sqrt{\tau}$ are therefore analysed. The dependence of cross-sections and distributions on the mass Q of the vector boson is also discussed at different energies $\sqrt{S}$ and the pattern of deviations from naive dimensional scaling is investigated. Particular attention is devoted to the tail of events at large q_T where a W/Z^0 is produced in association with hadronic jets. The probability of W/Z^0 production at $q_T > q_T^0$ is studied as a function of q_T^0 and $\sqrt{S}$. The behaviour of the average value of q_T, which is also determined by the large q_T tail, is evaluated at various values of τ and $\sqrt{S}$. Detailed predictions for W and Z^0 production at $\sqrt{S}$ = 630 GeV, the energy of the present run at the CERN collider are presented. Finally, ordinary Drell-Yan lepton pair production at the collider is also considered.

† Supported in part by the "Ministero della Pubblica Istruzione", Italy.

SECTION 1

INTRODUCTION

In a recent paper[1] we have re-examined the production of W and Z bosons at proton-antiproton colliders. We derived completely explicit expressions for the transverse momentum ($\vec{q}_T$) and the rapidity (y) distributions. These expressions, which are in a suitable form to be used as the input for numerical calculations, include the large amount of theoretical understanding of this process which has been accumulated over the last few years. A complete set of results was presented both for total and differential cross-sections including QCD radiative corrections. The analytic results for the transverse momentum (and rapidity) distributions have the following properties,

(a) at large q_T the correct behaviour resulting from the recoil against one parton[2,3] is automatically reproduced.

(b) in the region $q_T << Q$ ($Q = M_{W,Z}$) the soft gluon exponentiation is performed at the leading[4,5] and next to leading double logarithmic accuracy [6-9].

(c) after integration over q_T the known perturbative results for the total cross-sections (and $d\sigma/dy$)[10,11] are obtained including terms of order (α_s), (which give rise to the "K factors").

(d) all cross-sections are expressed in terms of quark distributions, which are precisely specified beyond the leading order. We choose the deep inelastic structure function F_2 as our reference distribution and evolve it to the appropriate scale Q.

In the present paper we explore the phenomenological implications of our previous treatment of vector boson production in more detail. We make numerical predictions which are (or will be) of considerable practical importance. We first discuss the production of W's and Z's at future super colliders with energies in the range $\sqrt{S}$ = (10-40) TeV. The extension of our formalism to this problem is complicated by the very small values of the scaling variable, $\sqrt{\tau} = M_W/\sqrt{S}$. This leads to two possible sources of problems. Firstly, the quark and gluon distributions are required at values of $x \sim \sqrt{\tau}$, much lower than those measured in deep inelastic scattering (or by W production at the CERN $Sp\bar{p}S$ collider). Secondly, in the treatment of the parton cross-section, we found that there are terms of order $(\alpha_s \ln^m(\frac{1}{\tau}))^n$. These terms, although not present order by order in the perturbative results, can be introduced by the resummation and exponentiation procedure if due care is not taken. The logarithms of τ become unacceptably large when $\sqrt{S}$ increases at fixed Q. We discuss both of these problems with special emphasis on the second one which is more specific to Drell-Yan type processes. Small values of τ are also encountered in ordinary lepton-pair production at the CERN collider where the mass of the lepton-pair is in the range Q = (10~20) GeV. We therefore consider also this case in some detail.

We then study the production cross-sections and q_T distributions of possible new heavy vector bosons, by varying the mass of the produced boson, but retaining the couplings of the ordinary charged W. This analysis is interesting, not only for the information it gives on the production of hypothetical heavy bosons, but also as a study of the

scaling properties of the various distributions. In the scaling limit dimensionless quantities should depend only on scaling variables and not on $\sqrt{S}$. For example, in the scaling limit one has,

$$S\,\sigma(Q,\sqrt{S}) = f(\tau) \tag{1}$$

$$q_T \frac{d\sigma(y=0)}{dq_T dy} \Big/ \frac{d\sigma(y=0)}{dy} = \Sigma(\tau, x_T) \tag{2}$$

with $x_T = 2q_T/\sqrt{S}$. We study the shape of $f(\tau)$ and $\Sigma(\tau,x_T)$ and the pattern of deviations from the scaling limit in the range $\sqrt{S} \approx (0.5\text{-}20.)$ TeV for reasonable values of τ and x_T. The scaling approximation is better for $f(\tau)$ than for $\Sigma(\tau,x_T)$. The deviation from scaling is especially noticeable in Σ, because the scale-breaking dependence on $\sqrt{S}/\Lambda$ and q_T/Λ (where $\Lambda=\Lambda_{QCD}$) is magnified by the exponentiation of the soft gluon emission.

We also calculated the number of events containing a W or a Z^o produced at large q_T. It is important to know the probability $\pi(q_T^o)$ for W/Z^o production with $q_T > q_T^o$ as a function of q_T^o (and also as a function of $\sqrt{S}$). The interest in this quantity stems from the fact that signals of new physics beyond the standard model are expected to show up at large q_T. Precise knowledge of $\pi(q_T^o)$ provides an estimate of the background at large q_T due to the physics of the standard model. This subject is especially topical since Z^o events at large q_T can appear as monojets[12] (i.e. one jet plus missing E_T) if the decay $Z^o \to \bar{\nu}\nu$ occurs. Similarly a W event at large q_T would be observed as an electron plus a jet[13] in an event with missing energy. Precisely these types of events have been reported by the UA1 and UA2 collaborations

respectively. Our conclusion, in qualitative agreement with other calculations,[14] is that the predicted rate of W or Z^0 production at the values of q_T required by the CERN events is too small to account for all the interesting events. Of course the comparison of an event rate probability with such a small number of events is rather premature. The conclusion will become definite if the same pattern of events remains even after greater statistics have been collected.

We first consider $\pi(q_T)$ at $\sqrt{S}$ = (540-630) GeV. Our determination of $\pi(q_T)$ at large q_T and $\sqrt{S}$ ~ 0.5 TeV proceeds in three steps. We first determine at what value of q_T the full transverse momentum distribution approaches the perturbative limit given by recoil against one parton. For $q_T \geq 30$ GeV the perturbative formula can be substituted for the more complicated expression which is valid at all values of q_T. This division of the range in q_T is approximately constant even as far up as $\sqrt{S}$ = 20 TeV because the onset of the perturbative region occurs when q_T is compatible with Q rather than with $\sqrt{S}$. We then evaluate $\pi(q_T)$ above this point in q_T from its perturbative expansion at order α_s. Particular attention is given to the estimation of the theoretical error on $\pi(q_T)$ at CERN collider energies. Because $\pi(q_T)$ is proportional to α_s the main source of error is lack of precision in the value of α_s coming from uncertainties in the value of Λ and the choice of scale (e.g. the choice between Q^2 and q_T^2). We therefore take advantage of the existing calculation[15] of the $q\bar{q}$ annihilation component of the q_T distribution at order α_s^2. At order α_s the quark-gluon component is found to give a smaller contribution than the quark-antiquark annihilation term at $\sqrt{S}$ = 0.5 TeV. It is therefore plausible that the quark-antiquark

annihilation term dominates over quark-gluon term also at order α_s^2. We have therefore repeated the calculation of $\pi(q_T)$ including the $O(\alpha_s^2)$ $q\text{-}\bar{q}$ contribution to the q_T distribution. Including these partial results from $O(\alpha_s^2)$ we find that the value of $\pi(q_T)$ is only slightly decreased, but that the theoretical error due to scale ambiguities is substantially reduced. We have also calculated $\pi(q_T)$ at large values of S up to $\sqrt{S}$ = 10 TeV. The perturbative calculations are still valid for $q_T \geq 30$ GeV in agreement with the expectation that the relevant parameter is the ratio of q_T and Q. The gluon distribution becomes more and more important with increasing $\sqrt{S}$, so at higher energies the $O(\alpha_s^2)$ results for $q\bar{q}$ alone cannot be reliably used.

The perturbative tail is also sufficient for a calculation of the average values of q_T and q_T^2 at high energy in a Drell-Yan type process.

$$\left\langle \left(\frac{q_T}{\sqrt{S}}\right)^m \right\rangle = \alpha_s(Q^2)\, h^{(m)}(\tau, \alpha_s(Q^2)) + \ldots \qquad (3)$$

where the dots indicate terms down by powers of $\sqrt{S}$. We computed $h^{(1)}$ and $h^{(2)}$ as a function of τ at energies in the range $\sqrt{S}$ = (0.5~100) TeV. We also computed $\langle q_T \rangle$ and $\sqrt{\langle q_T \rangle^2}$ for the case of W production. In this case the increase in $\sqrt{S}$ is to a large extent compensated by the corresponding decrease in τ so that $\langle q_T \rangle$ only varies in the range (7-22) GeV for $\sqrt{S}$ = (0.5-20) TeV.

Finally we give extensive results on q_T and y distributions for W/Z^0 production at $\sqrt{S}$ = 630 GeV, the energy of present CERN collider run, and for Drell-Yan lepton-pair production with Q = (10-20) GeV.

Numerical calculations are performed as described in detail in ref. 1. We ignore the smearing both from the intrinsic q_T of partons inside the nucleon and from possible initial state interactions between active and spectator quarks.[16] It is now known that the leading terms in the total production cross-sections are unchanged by initial state interactions.[17] However, a smearing effect could still possibly be present in the q_T distribution. The justification for neglecting these effects is that the average smearing momentum is less than $\langle q_T \rangle$ in the energy range of interest here. As a consequence, the slight flattening of the q_T distribution from the smearing falls within the present uncertainty from other sources. This has been checked numerically for smearing momenta below 1 GeV.

The values chosen for the boson masses are

$$M_W = 83.0 \text{ GeV} \quad , \quad M_Z = 93.8 \text{ GeV} \quad , \quad \sin^2\theta_W = 0.217 \tag{4}$$

The sensitivity of the numerical results to the choice of quark and gluon distributions in the proton (antiproton) was tested using different sets of parameterizations. We have used several sets of parton distributions. In various places in the paper we have used the sets given by Duke and Owens (DO)[18], the set proposed by Gluck, Hoffmann and Reya[19] (GHR), and the sets given by Eichten, Hinchliffe, Lane and Quigg (EHLQ)[20]. All three sets of distributions claim to be compatible with existing data from fixed target energies although they differ somewhat in the importance given to different experiments. For a comparison of the different distributions we refer the reader to ref.(20). The first set (DO1) has a smaller Λ

(Λ = 0.2 GeV) and a narrower gluon distribution at the evolution starting point Q_o^2 = 4 GeV^2. The second set (DO2) has Λ = 0.4 GeV and a broader gluon distribution. The third set (GHR) has Λ = 0.4 GeV. The distributions of Eichten et al.,which have the advantage that they are valid down to very small values of x, come both in a narrow glue version, EHLQ1 (Λ = 0.2 GeV) and a broad glue version EHLQ2 (Λ = 0.27 GeV). The full set of distributions is only used when the theoretical error is estimated. Otherwise we used as a reference one or other of the above parameterizations. In all cases the evolution is performed using only the lowest order evolution equation. Note that the value of Λ used for the Q^2 evolution of distributions is fixed by the authors of the different parameterizations. Thus, in a sense, they are only guaranteed to reproduce the existing data if used with the appropriate value of Λ. There are two numerical calculations in the present paper which require the running coupling to be specified to two loop accuracy. The first case is in the exponent of the soft gluon resummation which is treated to next to leading accuracy (for example, by including the Kodaira-Trentadue correction[6]). The second case occurs when the perturbative q_T distribution is improved by including the $O(\alpha_s^2)$ $q\text{-}\bar{q}$ contributions. In these two cases we have used the $\overline{MS}$ prescription and the two loop form of α_s, with $\Lambda_{\overline{MS}}$ = 200 GeV. However, we kept the evolution of parton distributions fixed as specified in (DO1) with the same value of Λ as for α_s.

The paper is organized as follows. In section 2 the basic formulae and results are recalled. In section 3 the production of vector bosons at super colliders is considered. In particular, an analysis of the

problems related to the small values of $\sqrt{\tau}$ is presented. Section 4 is devoted to total cross-sections and rapidity distributions. In section 5 the tail at large transverse momenta is studied, and the average transverse momentum $\langle q_T \rangle$ and $\pi(q_T^o)$, the probability of W/Z^o production at $q_T > q_T^o$, are evaluated. In section 6 detailed results for W/Z^o production at $\sqrt{S} = 630$ GeV are presented. Finally, section 7 contains a brief discussion of lepton-pair production at the CERN collider with $Q \ll M_{W,Z}$.

SECTION 2

BASIC FORMULAE AND RESULTS

In this section we give a summary of the main formulae and explain the derivation of the phenomenological results described in the following sections.

The total cross-section for vector boson production σ and the rapidity differential cross-section $d\sigma/dy$ are predicted by the QCD improved parton model[21] as an expansion in the strong coupling constant α_s. The corrections of order α_s to these cross-sections have been calculated and found to be important.[10,11] They increase the naive parton model prediction by an energy and rapidity dependent factor commonly referred to as the "K-factor". At fixed target energies the $O(\alpha_s)$ corrections are dangerously big and resummation techniques must be invoked[22] in an attempt to control the perturbation series. At collider energies and above their size is reduced because the coupling

constant is smaller. For the production of weak intermediate bosons at $\sqrt{S}$ = 0.5 TeV, they lead to a correction of about 30%. The total cross-section for W/Z production at collider energies is therefore more reliably predicted than the lepton pair production cross-section at fixed target energies.

The prediction of the entire boson transverse momentum distribution is more subtle, since all order effects always need to be taken into account. Renormalization group improved perturbation theory is valid when the transverse momentum q_T is of the same order as the vector boson mass Q. The large q_T tail of the transverse momentum distribution was one of the early predictions of the QCD improved parton model.[2,3] As q_T becomes less than Q, such that $\Lambda \ll q_T \ll Q$, a new scale is present in the problem and large logarithms of the form $\ln (Q^2/q_T^2)$ occur, forcing the consideration of all orders in α_s (because $\alpha_s(Q^2)\ln Q^2/q_T^2 \sim 1$). These terms are characteristic of a theory with massless vector gluons. Fortunately, these terms can be reliably resummed both in the leading double logarithmic approximation and beyond. This resummation was first attempted by Dokshitzer-Dyakonov-Troyan (DDT)[4] and subsequently modified and consolidated.[5] A consistent framework for going beyond the leading double logarithmic approximation has been indicated by Collins and Soper[8,9] (recently discussed and improved in ref. 23). The first subleading terms were given in ref. 6,7.

The combination of these results on the q_T distribution with the constraint on the area of the distribution provided by integrated cross-section at $O(\alpha_s)$, allows an essentially complete reconstruction of the q_T distribution to that accuracy. There is some uncertainty due to

the parton intrinsic transverse momentum but at collider energies it is present only in a restricted region at low q_T.

Schematically, for the $q\bar{q}$ annihilation term, the perturbative q_T distribution at order α_s is of the form,

$$\frac{d\sigma}{dq_T^2} = \sigma_o(1+A)\ \delta(q_T^2) + B\left(\frac{\ln\frac{Q^2}{q_T^2}}{q_T^2}\right)_+ + \frac{C}{(q_T^2)_+} + Y(q_T^2) \tag{5}$$

where σ_o is the lowest order cross-section and A, B and C are of order α_s or higher, and independent of q_T in the limit of fixed coupling α_s. $Y(q_T)$, which is also of order α_s, is a regular function of q_T at $q_T = 0$. The definition of the "plus" distribution is with respect to the kinematic upper limit of the q_T^2 integration,

$$\int_o^{A_T^2} g(x)\ f_+(x)\ dx = \int_o^{A_T^2} [g(x)-g(0)]\ f(x)dx \tag{6}$$

where $A_T = (q_T)_{MAX}$.

In particular the total cross-section is given by,

$$\sigma = \sigma_o(1+A) + \int_o^{A_T^2} Y(x)dx \tag{7}$$

Note that the integral of the B and C terms over the whole range of q_T^2 vanishes because of Eq. (6). These terms become large for $q_T << Q$ and have to be resummed to all orders. The q_T distribution in the exponentiated form is written as,

$$\frac{d\sigma}{dq_T^2} = Y(q_T^2) + \int\frac{d^2b}{4\pi}\, e^{-iq_T\cdot b}\, \sigma_o(1+A)\ \exp S(b) \tag{8}$$

where

$$S(b) = \int_0^{A_T^2} \frac{dk^2}{k^2} (J_o(bk)-1) \left(B \ln \frac{Q^2}{k^2} + C\right) \qquad (9)$$

The Bessel function J_o originates from the angular integration in d^2k and the subtraction resulting in the (J_o-1) factor is from the "plus" prescription defined in Eq. (6). The b transform is introduced in order to ensure the conservation of transverse momentum in multiple gluon emission.[21] Note that the integral over all values of q_T^2, which leads to the total cross-section, is given by,

$$\sigma = \int d^2b\, \delta^2(\vec{b})\, \sigma_o(1+A)\, \exp S(b) + \int_0^{A_T^2} dx\, Y(x)$$

$$= \sigma_o\,(1+A) + \int_0^{A_T^2} dx\, Y(x) \qquad (10)$$

in agreement with Eq. (7). The last step follows because $S(0) = 0$. We see that resummation alters the shape but not the normalisation of the cross-section since the whole tower of exponentiated terms gives no net contribution to the total cross-section.

Actually B (and C) in Eqs.(5,9) are known to a better accuracy than order α_s. The term of order α_s^2 in B was first derived in ref. 6. Recently it has been confirmed[7] using the results of ref. 15 for the perturbative q_T distribution from $q\bar{q}$ annihilation at order α_s^2. In the $\overline{MS}$ prescription for α_s one obtains,

$$B = +\frac{4}{3} \frac{\alpha_s(k^2)}{\pi} [1 + D\alpha_s(k^2) + \ldots] \qquad (11)$$

$$C = -2\,\frac{\alpha_s(k^2)}{\pi}\,[1 + E\alpha_s(k^2) + \ldots\ldots] \tag{12}$$

where[6,7]

$$D = \frac{1}{2\pi}\,[\frac{67}{6} - \frac{\pi^2}{2} - \frac{5}{9}\,n_f] \tag{13}$$

The value of E is also known[7], but is less important because the whole C term is suppressed by a large logarithm with respect to the B term. After the integration over k^2 in Eq. (9) is performed, the term D multiplies a factor of order $\alpha_s^2(Q^2)\ln^2 Q^2$, which approaches a constant for $Q^2 \to \infty$. Thus the effect of D, although suppressed by a logarithm with respect to the leading term, persists at all Q^2.

When the dependence on the rapidity y is also taken into account the final result is given by,

$$\frac{d\sigma}{dq_T^2 dy} = N\,\{\int \frac{d^2b}{4\pi}\,e^{-iq_T\cdot b}\;\; R(b^2,Q^2,y)\cdot \exp S(b^2,Q^2,y) + \\ + Y(q_T^2,Q^2,y)\;\} \tag{14}$$

where $S(b^2,q^2,y)$ is given by Eqs. (9),(11-13), with

$$A_T^2 = A_T^2(y) = \frac{(S+Q^2)^2}{4\,S\,\cosh^2 y} - Q^2 \tag{15}$$

We display here the explicit form of R which will be needed later. This term is the generalisation to the y dependent case of the factor $\sigma_o(1+A)$ in Eq. (8).

$$R(b^2,Q^2,y) = H(x_1^o,x_2^o,P^2)\ [1 + \frac{\alpha_s}{2\pi}\frac{4}{3}\ (-3\ \ln\frac{A_T^2}{Q^2} - \ln^2\frac{A_T^2}{Q^2}\ )]$$

$$+ \frac{\alpha_s}{2\pi}\frac{4}{3}\ [\int_{x_1^o}^1 \frac{dz}{z}\ f_q(z)\ H(x_1^o/z,\ x_2^o) + \int_{x_2^o}^1 \frac{dz}{z}\ f_q(z)\ H(x_1^o,x_2^o/z)]$$

$$+ \frac{\alpha_s}{2\pi}\frac{1}{2}\ [\int_{x_1^o}^1 \frac{dz}{z}\ f_g(z)\ K_2(x_1^o/z,\ x_2^o) + \int_{x_2^o}^1 \frac{dz}{z}\ f_g(z)\ K_1(x_1^o,x_2^o/z)] \quad (16)$$

In this expression $H \sim q(x_1)\ \bar{q}(x_2)$, $K_1 \sim [q_1(x) + \bar{q}(x_1)]\ g(x_2)$ and $K_2 \sim [q(x_2) + \bar{q}(x_2)]\ g(x_1)$ contain the appropriate bilinear combinations of parton distributions, f_q and f_g are known kernels (Eqs. (59) of ref. 1) and P^2 is a precisely defined scale of order q_T^2 (Eq. 58 of ref. 1). As usual $x_{1,2}^o = \sqrt{\tau}\ e^{\pm y}$. The regular term $Y(b^2,Q^2,y)$ in Eq. (14) is divided into the parts due to the annihilation and Compton scattering graphs which can be found in Eqs. (62,63,64) of ref.(1).

The y distribution is obtained by integration over q_T^2 of Eq. (14) and reproduces the known perturbative results correct up to and including order α_s. The y distribution is given by Eqs. (80-86) of ref. (1). Alternative, but identical, expressions for $d\sigma/dy$ can be found in ref. (10) and (24). Here we only report the very simple perturbative formula for the total cross-section.

$$\sigma = N \int \frac{dx_1 dx_2}{x_1 x_2}\ [H(x_1,x_2,Q^2)[\delta(1-\frac{\tau}{x_1x_2}) + \frac{\alpha_s}{2\pi}\frac{4}{3}\ \theta(x_1x_2-\tau)2f_q^T(\frac{\tau}{x_1x_2})$$

$$+ \frac{\alpha_s}{2\pi}\frac{1}{2}\ \theta(x_1x_2-\tau)\cdot\left(K_1(x_1,x_2,) + K_2(x_1,x_2)\right) f_g^T(\frac{\tau}{x_1x_2})] + \quad O(\alpha_s^2) \quad (17)$$

The kernels $f_{q,g}^T$ are given in Eq. (88) of ref. 1.

SECTION 3

W AND Z PRODUCTION AT SUPER COLLIDERS.

In this section we consider W/Z^{o} production at centre of mass energies in the range $\sqrt{S}$ = (10-20) TeV. The results of this analysis are clearly relevant for the experiments to be set up in the next decade. However, as already mentioned, this problem is also interesting in its own right because it provides an example of the QCD improved parton model as applied to Drell-Yan type processes at very small values of τ. In this context it is important to note that the present collider offers an ideal configuration for the application of QCD to vector boson production. The relevant values of $\sqrt{\tau}$ for $\sqrt{S}$ = (540-630) GeV are in the range,

$$\sqrt{\tau} = 0.13 \sim 0.17 \tag{18}$$

The quark and gluon distribution functions are well known for the values of τ in Eq. (18). By way of contrast if we extrapolate to $\sqrt{S}$ = 20 TeV we find that $\sqrt{\tau} \approx 5 \cdot 10^{-3}$. At these values of Q and $\sqrt{\tau}$ the Drell-Yan total cross-sections σ and $d\sigma/dy$ are dominated by sea-quark distributions. Although the gluon distribution is much larger than the quark distribution at small x, the gluon contribution to σ and $d\sigma/dy$ remains relatively small even at super collider energies. The contribution to σ or $d\sigma/dy$ from gluon distributions enters through the Compton graph, and is suppressed by a factor of order $3/8\ \alpha_s(Q^2)/\pi$ with respect to the lowest order annihilation term. On the other hand the gluon distribution is important for $d\sigma/dq_T dy$ at large q_T where the

cross-section itself is very small.

At such small values of x, neither the sea quark nor the gluon distributions can be obtained directly from existing experiments. They are normally estimated at low x and large Q^2 from the quark and gluon distribution functions at larger x and smaller Q^2 using the QCD evolution equations. When ln(1/x) is large the one loop evolution equations are dominated by the poles at x = 0 which appear in the splitting functions[25], (C_F=4/3, C_A=3, n_f=no. of flavours).

$$P_{gg}^{(1)}(x) \underset{x\to 0}{\simeq} \frac{\alpha_s}{2\pi}\frac{2C_A}{x} \; ; \quad P_{gq}^{(1)}(x) \underset{x\to 0}{\simeq} \frac{\alpha_s}{2\pi}\frac{2C_F}{x} \tag{19}$$

The small x behaviour of the gluon distribution is driven by $P_{gg}(x)$. In the basis $\begin{pmatrix}\Sigma\\ g\end{pmatrix}$ the evolution of the moments is controlled by the anomalous dimension matrix, which near n = 1 has the form,

$$A_n = \frac{\alpha_s}{2\pi}\begin{pmatrix} 0 & \frac{4}{3}n_f \\ \frac{2C_F}{(n-1)} & \frac{2C_A}{(n-1)} \end{pmatrix} \tag{20}$$

This implies that the growth of the singlet quark distribution Σ in the small x region is less rapid than the growth of the gluons. Denoting by $\Gamma(x)$ the momentum distribution of the gluons,

$$\Gamma = xg \tag{21}$$

we obtain that,

$$Q^2 \frac{d\Gamma(x,Q^2)}{dQ^2} = \frac{\alpha_s(Q^2)C_A}{\pi} \int_x^1 \frac{dz}{z} \Gamma(z,Q^2) \tag{22}$$

Setting,

$$\xi = b \int^{Q^2} \frac{dk^2}{k^2} \alpha_s(k^2) = \ln(\ln \frac{Q^2}{\Lambda^2}) \tag{23}$$

$$y = \frac{2C_A}{\pi b} \ln \frac{1}{x} \tag{24}$$

where $[b\alpha_s(Q^2)]^{-1} = \ln Q^2/\Lambda^2$, Eq. (22) can be cast in the form [26,27]

$$\frac{d^2\Gamma(y,\xi)}{d\xi dy} = \frac{1}{2} \Gamma(y,\xi) \tag{25}$$

The solution to this equation for large ξy is given by

$$\Gamma(y,\xi) = \exp\sqrt{2\xi y} \tag{26}$$

which expressed in terms of the gluon distribution is [26,27]

$$g(x) = \frac{1}{x} \exp \sqrt{\frac{4C_A}{\pi b} \ln \ln \frac{Q^2}{\Lambda^2} \ln \frac{1}{x}} \tag{27}$$

The small x behaviour of the timelike splitting functions is also given by Eq. (19). The above solution to the one loop evolution equation in the small x region would appear to be valid both for parton distributions in the spacelike region and fragmentation functions in the timelike region. If it were valid at x = 0 for fragmentation functions if would imply a behaviour for the multiplicity which is known not to be the correct QCD prediction. In the timelike region it is known that the

behaviour of the anomalous dimension near n = 1 is modified by higher order terms which were not included in the above analysis,[28]

$$\gamma_n^{GG}(\alpha) = \frac{\alpha C_A}{\pi}\frac{1}{n-1} - 2\left(\frac{\alpha C_A}{\pi}\right)^2 \frac{1}{(n-1)^3} + \ldots\ldots$$

$$= \frac{1}{4}\left[-(n-1) + \sqrt{(n-1)^2 + \frac{8\alpha C_A}{\pi}}\right] \qquad (28)$$

In x space this is equivalent to the occurence of terms of order $\alpha_s/x[\alpha_s \ln^2(1/x)]^{m-1}$ in m^{th} order perturbation theory. These terms modify the behaviour of the $\gamma_n^{GG}(\alpha)$ near n = 1 into a non-singular one. The true large Q^2 prediction for the multiplicity is given by

$$\bar{n}(Q^2) = n_o \exp \int_\alpha^{\alpha(Q^2)} d\alpha \frac{\bar{\gamma}^{GG}(\alpha)}{\beta(\alpha)} = n_o \exp \sqrt{\frac{2C_A}{\pi b} \ln \frac{Q^2}{\Lambda^2}} \qquad (29)$$

The subleading corrections to this expression have also been calculated in ref. 29.

The question which we wish to address here is whether or not the higher order terms in the spacelike anomalous dimensions modify the behaviour given by Eq. (27). The full answer to this question is not known but the properties of higher order corrections to the spacelike anomalous dimensions which are known, imply that Eq. (27) is the correct asymptotic behaviour in the range of x of current interest. The form of the two loop anomalous dimension matrix in the small x region is [30]

$$P^{(2)}_{x\to 0} \left(\frac{\alpha_s}{2\pi}\right)^2 \begin{pmatrix} \frac{40}{9}\frac{C_F T_R n_f}{x} & \frac{40}{9}\frac{C_A T_R n_f}{x} \\ \frac{C_F C_A}{x} - \frac{40}{9}\frac{C_F T_R n_f}{x} & \frac{4}{3x}(C_F - \frac{C_A}{2})\, T_R n_f - \frac{40}{9x} C_A T_R n_f \end{pmatrix} \tag{30}$$

In contrast to the timelike case we see that the terms of order $\alpha_s/x[\ln(1/x)]^m$ for $m = 1$ and 2 are absent. Indeed it is known[31] to all orders that the most singular terms in the series for the anomalous dimension are of the form,

$$\gamma_n^{GG}(\alpha) = \sum_{j=1}^{\infty} a_j \left(\frac{\alpha_s C_A}{\pi(n-1)}\right)^j \tag{31}$$

where

$$a_1 = 1,\ a_2 = 0\ \ a_3 = 0\ \ a_4 = 2\xi(3),\ \ldots . \tag{32}$$

and $\xi(3)$ is Riemann zeta function. The second and third order terms are less singular than might be expected from the general series Eq.(31). We therefore conclude that the asymptotic behaviour predicted by the one loop evolution equations [Eq. (27)] should be valid down to much smaller x in the spacelike region than in the timelike region. For fragmentation functions it breaks down when $C_A\alpha_s/\pi \ln^2(1/x) \approx 1$, whereas for the gluon distribution function it only breaks down when $C_A\alpha_s/\pi \ln(1/x) \approx 1$. The ordinary evolution equations are therefore suitable for a description of the singlet distributions at least down to $x \approx 10^{-3}$ for $Q < 1$ TeV. The behaviour at still smaller values of x has been studied in ref.(26).

The only remaining problem with regard to the parton distribution functions at low x is to convince ourselves that the parameterisations which we use provide an accurate description of the behaviour predicted by the QCD evolution equation in the region of x at which we use them. For the distributions of Duke and Owens the discrepancies between the fitted values and the results of the evolution program are stated[18] to be nowhere more than a few percent for $x > 5 \cdot 10^{-3}$ and $Q < 1$ TeV. On the other hand the GHR parameterisation[19] is valid for $x \geq 10^{-2}$ and $Q \leq 2 \cdot 10^{2}$ GeV. The EHLQ distributions are valid for $x > 10^{-4}$ and $Q < 10$ TeV. In Fig. 1 the DO1, GHR and EHLQ1 sets of distributions at $Q \sim 83$ GeV are shown for $x \geq 10^{-3}$. We see that they are quite similar for $x \geq 5 \cdot 10^{-3}$, i.e. in the region of interest for most of this paper. In Fig. 2 we report, as a further check, the bilinear combinations of distributions $H \sim q\bar{q}$ and $K \sim (q+\bar{q}) \cdot g$ which are directly relevant for W production, computed from DO1, GHR and EHLQ1 as functions of $\sqrt{\tau}$.

Even if the parton distributions at small x are given one is still faced with the problem of treating the relevant parton subprocesses correctly in the region of small τ. The massive vector boson in Drell-Yan processes enters in a totally inclusive final state. The well known theorem[32] on mass singularities ensures that all such singularities which might be present in the Drell-Yan total cross-section can be included in the initial state, i.e. factorised into the parton distributions. We expect that all singularities for $\tau \to 0$ are removed once the parton distributions are taken from Deep inelastic scattering and evaluated at the scale Q^2. This is what happens in explicit calculations at order α_s as we shall now illustrate.

To simplify the discussion we assume that the parton distributions effectively behave like 1/x at small values of x. The lowest order terms of σ and $d\sigma/dy$ then behave at small τ as follows

$$\sigma_o \sim \int_\tau^1 \frac{dx}{x} H(x, \frac{\tau}{x}) \sim \frac{1}{\tau} \ln \frac{1}{\tau} \tag{33}$$

$$\frac{d\sigma_o}{dy} \sim H(x_1^o, x_2^o) \sim \frac{1}{\tau} \tag{34}$$

Note that the total rapidity range increases like $\ln(1/\tau)$ at small τ in agreement with Eqs. (33),(34). The double differential cross-section in q_T^2 and y reduces to a δ-function term in lowest order,

$$\frac{d\sigma_o}{dq_T^2 dy} \approx H(x_1^o, x_2^o)\ \delta(q_T^2) \sim \frac{1}{\tau}\ \delta(q_T^2) \tag{35}$$

It is simple to check that the correction terms of order α_s to σ and $d\sigma/dy$ behave at small τ in the same way as the lowest order terms. This is immediately seen from Eq. (17) for the total cross-section corrected at order α_s. The correction to the $q\bar{q}$ term behaves at small τ as,

$$d\sigma_q \approx \alpha_s \frac{1}{\tau} \ln \frac{1}{\tau} \int_{\sqrt{\tau}}^1 dz\ f_q^T(z) \tag{36}$$

Since $f_q^T(z)$ is integrable at z=0, the lower limit of integration can be replaced by zero. The correction from the QCD Compton term also behaves in exactly the same way and the stated result follows.

The corresponding result for $d\sigma/dy$ and $d\sigma/dq_T^2 dy$ is also true, although it may superficially seem that terms proportional to $\alpha_s \ln^2(1/\tau)$ and $\alpha_s \ln(1/\tau)$ are present in Eqs. (14-16) of this paper and in Eqs. (80-86) of ref. 1. A careful examination shows in fact that the dangerous terms cancel exactly.

In order to extrapolate the resummed expression for $d\sigma/dq_T^2 dy$ to small τ the exponentiation must be performed in such a way that no spurious $[\alpha_s \ln^m(1/\tau)]^n$ terms, with $m = 1,2$ appear at order $n \geq 2$. For this purpose, as already mentioned in ref. 1, the exponential in Eqs. (9-14) must be transformed according to,

$$\exp S = \exp \int_0^{A_T^2} \approx (1 + \int_{Q^2}^{A_T^2}) \exp \int_0^{Q^2} \tag{37}$$

where A_T is given by Eq. (15). For normal values of τ this replacement is numerically insignificant because the large transverse momenta between Q and A_T are always in the perturbative region. But for very small τ the integral from Q^2 to A_T^2 produces large logarithms and the difference between the two sides of Eq.(37) becomes important. The proposed replacement eliminates these large logarithms by cancelling them against the large logarithms appearing in the factor R in Eq. (14), which is given in Eq. (16). Including also the factor R one obtains,

$$R \exp S = R \left(1 + \int_{Q^2}^{A_T^2}\right) \exp \int_0^{Q^2} =$$

$$\left\{H(x_1^o, x_2^o, P^2) \left[1 + \frac{2\alpha_s(P^2)}{3\pi} \left(-3 \ln \frac{A_T^2}{Q^2} - \ln^2 \frac{A_T^2}{Q^2}\right)\right] + r\right\}$$

$$\left[1 + \frac{2}{3\pi} \int_{Q^2}^{A_T^2} \frac{dk^2}{k^2} \alpha_s(k^2) \left(J_o(bk)-1\right) \left(-3 + 2 \ln \frac{Q^2}{k^2}\right)\right] \cdot \exp \int_o^{Q^2} \qquad (38)$$

Here r contains all terms in R without large logarithms and P^2 is a scale of order q_T^2. It is immediately seen that the large logarithms of order α_s cancel. By dropping terms of order α_s^2 we finally write,

$$R \exp S = \left[H(x_1^o, x_2^o, P^2) + r\right]$$

$$\left[1 + \frac{2}{3\pi} \int_{Q^2}^{A_T^2} \frac{dk^2}{k^2} \alpha_s(k^2) \; J_o(bk) \left(-3 + 2 \ln \frac{Q^2}{k^2}\right)\right] \exp \int_o^{Q^2} \qquad (39)$$

Note that for $b = 1/q_T$ the Bessel function suppresses the integral by oscillating for $q_T \geq Q$. Also observe that the total cross-section at order α_s is not altered by the modification given in Eq. (37). Using Eq. (37) the q_T distribution of Drell-Yan processes can be safely extrapolated down to small values of τ provided that the parton distributions are known at the relevant values of $x = (\sqrt{\tau})$.

In conclusion, the perturbative expansion remains valid for σ and $d\sigma/dy$ even at very small values of τ. The only limitation in predicting σ and $d\sigma/dy$ at small $\sqrt{\tau}$ arises from our ignorance of parton

distributions at small x. The extrapolations of sea and gluon distributions to small x and large Q^2, obtained from the data at larger x and smaller Q^2 by using the QCD evolution equations, can be trusted until $C_A\alpha_s/\pi \ln(1/x) \leq 1$. The crucial feature is the absence in the spacelike case of terms in the perturbation series of order $C_A\alpha_s/\pi \ln^2(1/x)$. This permits sensible predictions to be made down to $x \sim 10^{-3}$ for $Q \sim (0.1\text{-}1)$ TeV. The same conclusion also applies to the transverse momentum distribution $d\sigma/dq_T^2dy$ if and only if the resummation of soft gluon emission is implemented without introducing spurious large logarithms in the small τ region. The resulting expression given in Eq. (39) satisfies this additional important requirement together with the properties listed in the introduction.

In Fig. 3 we plot the resulting normalised q_T distributions for W/Z production in the range of energies between the present collider (see also Fig. 13) and $\sqrt{S} = (10\text{-}20)$ TeV. The distribution becomes flatter as the energy increases, but much less than would be expected from a simple rescaling of the average q_T. We shall in fact see in section 5, where $\langle q_T \rangle$ is computed and discussed in detail, that when $\sqrt{S}$ is increased at fixed Q the rise of $\langle q_T \rangle$ is slowed down by the effect of the decrease in τ.

We conclude this section by briefly discussing the scaling properties of the q_T distribution. In the naive parton model the dimensionless quantity,

$$\Sigma = \frac{q_T \frac{d\sigma(y=0)}{dq_T dy}}{\frac{d\sigma}{dy}(y=0)} \tag{40}$$

is only a function of τ and x_T, ($\Sigma = \Sigma(\tau, x_T)$ with $x_T = 2q_T/\sqrt{S}$). This is no longer true in the QCD improved parton model. The results for Σ which are obtained from the complete QCD calculation in the range of energies $\sqrt{S}$ = (0.63-10) TeV with $\sqrt{\tau} = 0.13$ are shown in Fig. 4. As is seen the scaling violations are quite substantial, but the scaling approximation can still be very useful for a qualitative understanding of the dependence of the q_T distribution on Q and $\sqrt{S}$.

SECTION 4

TOTAL CROSS-SECTION AND RAPIDITY DISTRIBUTIONS

In this section we shall present results on total cross-sections and rapidity distributions for the production of W and Z vector bosons. We also consider the possibility of heavier W bosons. Our results are presented for energies in the range $\sqrt{S}$ = (0.63-40.TeV). The total cross-section is computed from Eq. (17) which includes the $O(\alpha_s)$ corrections and the rapidity distribution $d\sigma/dy$ is obtained from a similar $O(\alpha_s)$ expression given by Eqs. (80-86) of ref. 1.

In Table 1 we give the values of $\sigma^{W^+ + W^-}$ and σ^{Z^0}, together with an estimate of the associated theoretical error, at significant values of the centre of mass energies. The error is obtained by varying the sets

of parton distributions, the value of Λ and also the choice of $\alpha_s(\langle q_T^2 \rangle)$ or $\alpha(Q^2)$ in the first order terms. In Fig. 5 we plot the total cross-sections for W production as a function of energy for both proton antiproton and proton-proton colliders. Because of the dominance of the sea quarks at small x the two cross-sections are practically identical at high energy. Also shown in Fig. 5 are the cross sections for production of possible heavier W's, obtained by varying M_W with fixed couplings. This is also important as a study of the scaling violations in the total cross-section shown in Fig. 6. In the scaling limit the dimensionless quantity S_0 is independent of S at fixed τ. The scaling violations, almost invisible in the double logarithmic plot, are quite sizeable in reality.

The evolution of the y distribution for W/Z^o production as a function of energy is shown in Fig. 7. We see that the W's are more and more produced in the forward (or backward) direction as the energy increases. However, the central region is where proportionally heavier W's would be produced. In fact, we also see from Fig. 7 that the y distribution is not much changed by going to high energy with fixed τ. In other words, the scaling violations in these normalised y distributions at fixed τ are small. Figs. 5, 6 and 7 were obtained using a fixed set of parton distribution functions and are subject to theoretical errors of the size indicated in Table 1.

SECTION 5

LARGE TRANSVERSE MOMENTA

In this section we study the large transverse momentum tail of the q_T distribution. As already mentioned in the introduction this is especially important in the search for new physics beyond the standard model. In fact W and/or Z^o production at large q_T could cause events with "monojets" or "lepton(s) plus jet(s)", in addition to missing E_T. These are typical triggers in the search for new phenomena.

We shall focus our attention on the quantity $\pi(q_T)$ defined as the probability of W/Z production with transverse momentum larger then q_T,

$$\pi(q_T) = \int_{q_T}^{A_T(o)} \frac{d\sigma(y=0)}{dp_T dy}\, dp_T \;/\; \int_{o}^{A_T(o)} \frac{d\sigma(y=0)}{dp_T dy}\, dp_T \qquad (41)$$

where $A_T(y)$ is given in Eq. (15). We shall also consider the behaviour of the average transverse momentum at zero rapidity $\langle q_T \rangle$ (and $\sqrt{\langle q_T^2 \rangle}$):

$$\langle q_T \rangle = \int_{o}^{A_T(o)} q_T \frac{d\sigma(y=0)}{dq_T dy}\, dq_T \;/\; \int_{o}^{A_T(o)} \frac{d\sigma(y=0)}{dq_T dy}\, dq_T \qquad (42)$$

as a function of energy and τ. Both $\langle q_T \rangle$ and $\pi(q_T)$ (at large q_T) are fixed by the perturbative tail of the q_T distribution. In the naive parton model $\langle q_T \rangle$ is a constant in energy at fixed τ. In the QCD improved parton model $\langle q_T \rangle$ increases with $\sqrt{S}$, according to Eq. (3). At fixed τ the increase is linear, up to logarithmic corrections, with a slope which is proportional to $\alpha_s(Q^2)$ in lowest order perturbation

theory. The slope can be computed in perturbation theory because the average q_T value is determined by the events in the small but long tail at large q_T which extends up to $A_T \sim \sqrt{S}/2$ [see Eq. (15)].

By construction, the final expression for $d\sigma/dq_T^2 dy$ in Eq. (14) [with or without the modification in Eq. (39)] approaches the correct perturbative value when terms of order α_s^2 are negligible. Thus, in principle, one could use the exact expression for the computation of $\pi(q_T)$ and $\langle q_T \rangle$. However, the perturbative expressions are simpler to handle numerically. For sufficiently large q_T and a fixed amount of computer time one obtains a far better numerical precision on $\pi(q_T)$ by working directly with the perturbative expression. Similarly the perturbative formulae are also more efficient for computing the behaviour of $\langle q_T \rangle$ as a function of $\sqrt{S}$ and τ. The complete q_T distribution can then be used to check at a few points that the soft radiative contribution can indeed be neglected.

The value of q_T at which the q_T distribution is well described by the perturbative tail alone can be read from Figs. 8,9. The result is that the perturbative tail is a quite adequate description of the actual q_T distribution for W/Z^0 production provided that $q_T \geq 30$ GeV, almost independent of $\sqrt{S}$ in the range $\sqrt{S} \approx 0.5\text{-}20$ TeV (in agreement with the fact that the perturbative expression is expected to hold at $q_T \sim Q$).

In table 2 we report the values of $\pi(q_T)$ for $q_T \geq 25$ GeV for W and Z^0 production at $\sqrt{S} \approx (540\text{-}630)$ GeV, as calculated from the perturbative q_T distribution at order α_s, normalised by the lowest order cross-section (as is correct when terms of order α_s^2 are neglected). We prefer relative probabilities rather than absolute rates. From the

probabilities one can more easily obtain the fraction of W/Z expected at large q_T from the total number of W/Z observed, (assuming that the experimental acceptance is independent of q_T). The main source of the error quoted in table 2, apart from the uncertainties on the parton distributions, is from the value of α_s. Without including terms of order α_s^2 one cannot decide whether to use $\alpha_s(q_T^2)$ or $\alpha_s(Q^2)$ or another comparable scale. Taken together with the ambiguities on the value of Λ, the overall uncertainty on α_s is responsible for most of the quoted error, because $\pi(q_T)$ is proportional to α_s at this order.

To proceed further in the theoretical accuracy one should include all terms of order α_s^2 in the perturbative q_T distribution (and normalise by the integrated cross-section with the $O(\alpha_s)$ correction included). A complete calculation of the q_T distribution at order α_s^2 has not yet been done. However, the contribution at order α_s^2 from the $q\bar{q}$ annihilation diagrams has been evaluated.[15] Presumably this is the most important term, because the QCD Compton contribution at order α_s is small at $\sqrt{S} \sim 0.5$ TeV relative to the dominant $q\bar{q}$ term of the same order. We have thus included the $q\bar{q}$ corrections at order α_s^2 in the numerator and the complete $O(\alpha_s)$ cross-section in the denominator. The results for $\pi^W(q_T)$ at $\sqrt{S} = 0.54$ TeV are given in Table 3. The central value of $\pi(q_T)$ is slightly lowered because the shift in the numerator is of equal sign but smaller than the change in the denominator (the latter being due to the "K-factor"). The main advantage of including the terms of order α_s^2 is that they lead to a somewhat smaller error, because the scale ambiguity in α_s is displaced to the terms of $O(\alpha_s^2)$. The form of the $O(\alpha_s^2)$ corrections varies according to the choice made for the scale

of the coupling in the linear terms in such a way as to compensate for the variations up to terms of $O(\alpha_s^3)$. The quoted theoretical error in Table 3 does not include the neglect of all the parton diagrams of $O(\alpha_s^2)$ except the $q\bar{q}$ contribution.

From the values of $\pi^{W,Z}(q_T)$ at $\sqrt{S}$ = 0.54 TeV we see, for example, that it is quite unlikely to find more than 3% of W and Z^o production with an associated jet of $q_T \geq 35$ GeV. In particular taking into account a factor ~6 between $\Gamma(Z \to \Sigma_i \bar{\nu}_i \nu_i)$ and $\Gamma(Z \to e^+e^-)$, it follows that we expect 18% as many "monojets" with $q_T \geq 35$ GeV as observed $Z^o \to e^+e^-$ events.

Finally in Table 4 we report the values of $\pi^W(q_T)$ at $\sqrt{S}$ = 1.6 TeV and 10 TeV, at order α_s, for a given set of parton distributions and a given choice of scale for α_s [i.e. $\alpha_s = \alpha_s(Q^2)$].

We now consider the average value of transverse momentum for W production as a function of $\sqrt{S}$ and of τ (i.e. we assume the existence of new W's with the same couplings but different masses than the ordinary W. The τ dependence obtained in this way is essentially the same as that obtained for Z^o production and in the production of lepton pairs. In Figs. (10,11,12) we plot $\langle q_T \rangle$ and $\sqrt{\langle q_T^2 \rangle}$ for $\sqrt{S}$ = (0.54-20) TeV and $\sqrt{\tau}$ = 0.01 - 0.3. Fig. 12 refers to proton-proton collisions. Also plotted in Figs. 10,11 are the values of $\langle q_T \rangle_W$ and $\sqrt{\langle q_T^2 \rangle_W}$ for the ordinary W. One sees that the τ dependence is very pronounced but that the variation of the $\langle q_T \rangle$ slope with $\sqrt{S}$ is quite mild. This change of slope with $\sqrt{S}$ is definitely present but hard to discern on a log-log plot. At $\sqrt{S}$ = 20 TeV the average value of the W transverse momentum is about 22 GeV.

SECTION 6

W AND Z^0 PRODUCTION AT $\sqrt{S}$ = 630 GeV

The forthcoming run at the CERN collider will be at $\sqrt{S} = 0.63$ TeV. It is therefore useful to give detailed predictions for this particular energy. We shall give our results for W production. It is important to emphasize that the predicted shape of the suitably normalised transverse momentum distributions for W and Z production are practically the same. The difference between W and Z^0 in normalised distributions is marginal and in most cases falls within the limits of the theoretical uncertainty.

The main results are collected in Table 5, where the quantity $(1/\sigma)/(d\sigma/dq_T dy)$ is given for different values of q_T and y, for our reference set of distributions and $\alpha_s = \alpha_s(Q^2)$. Figs. 13,14 also refer to the same set of results. Fig. 13 shows the normalised q_T distributions at different fixed values of y. The q_T distribution obviously becomes softer for increasing y. The differences in the q_T distributions for different y which are visible in Fig. 13 provide a measure of the limits of the often used approximation of a factorised form for the y and q_T distributions. As a first approximation the factorised form is acceptable for $y \leq 1$. On the other hand we see from Fig. 14 that the rapidity distribution $d\sigma/dy$ is not sufficiently peaked near y=0 to make the tail of events at $y > 1$ unimportant.

SECTION 7

LEPTON PAIR PRODUCTION BELOW THE W AND Z^0 MASS AT THE COLLIDER.

The experimental study of Drell-Yan lepton pairs at collider energies is interesting because it tests the QCD description of Drell-Yan processes for values of $\sqrt{\tau}$ in the range $\sqrt{\tau} \sim 10^{-2}$–10^{-1}. The background of lepton pairs from heavy flavour production can be estimated[33] and is especially important at small values of Q.

In Fig. 15 we plot the total cross-section for $\sqrt{S} = 540$ GeV as a function of Q. Only the virtual photon contribution is included. The following values of the integrated cross-section were obtained:

$$\sigma(Q > 12 \text{ GeV}) = (230 \pm 70)\text{pb} \quad (43)$$

$$\sigma(Q > 16 \text{ GeV}) = (110 \pm 35)\text{pb} \quad (44)$$

$$\sigma(Q > 20 \text{ GeV}) = (\ 50 \pm 20)\text{pb} \quad (45)$$

where the theoretical error, obtained by variation of parameters and sets of parton distributions, is also indicated.

The normalised y distributions for different values of Q are shown in Fig. 16. Finally the normalised q_T distributions are plotted in Fig. 17 for the same values of Q. Fig. 17 was obtained using the formulae of ref.(1), incorporating the modification Eq.(37).

CONCLUSIONS

In this paper we have investigated the production of W's, Z's and virtual photons in hadron hadron collisions using the basic parton parton annihilation mechanism. Using formulae, presented in ref.(1), which are the result of many years of theoretical work, we have made numerical predictions for present and future collider energies. In doing so we have also attempted to estimate the uncertainties due to our lack of precise knowledge of the input parameters. The predictions test many aspects of the standard SU(3)xSU(2)xU(1) model. We must now await the response of experiment.

Acknowledgements

This work was performed while one of us (G. M.) was visiting CERN. The hospitality of the CERN Theory group is gratefully acknowledged.

References

1. G. Altarelli, R. K. Ellis, M. Greco and G. Martinelli, Nucl. Phys. B246 (1984) 12.

2. G. Altarelli, G. Parisi, and R. Petronzio, Phys. Lett. 76B (1978) 351,356

3. H. Fritzsch, and P. Minkowski, Phys. Lett. 74B (1978) 384;
K. Kajantie and R. Raitio, Nucl. Phys. B139 (1978) 72;
F. Halzen and D. M. Scott, Phys. Rev. D18 (1978) 3378;
See also, P. Aurenche and J. Lindfors, Nucl. Phys. B185 (1981) 274.

4. Yu. L. Dokshitzer, D. I. Dyakonov and S. I. Troyan, Phys. Lett. 78B (1978) 290; Phys. Rep. 58 (1980) 269.

5. G. Parisi and R. Petronzio, Nucl. Phys. B154 (1979) 427.
G. Curci, M. Greco and Y. Srivastava, Phys. Lett. 43 (1979) 434; Nucl. Phys. B159 (1979) 451.

6. J. Kodaira and L. Trentadue, Phys. Lett. 112B (1982) 66; 123B (1983) 335.

7. C. T. H. Davies and W. J. Stirling, Nucl. Phys. B244 (1984) 337;
C. T. H. Davies, B. R. Webber, W. J. Stirling, CERN-TH 3987/84.

8. J. C. Collins and D. E. Soper, Nucl. Phys. B193 (1981) 381; B194 (1982) 4445; B197 (1982) 446.

9. S. C. Chao and D. E. Soper, Nucl. Phys. B214 (1983) 405;
S. C. Chao, D. E. Soper and J. C. Collins, Nucl. Phys. B214 (1983) 513.

10. G. Altarelli, R. K. Ellis and G. Martinelli, Nucl. Phys. B143 (1978) 521; (E) B196 (1978) 544; B157 (1979) 461.

11. J. Kubar-Andre and F. E. Paige, Phys. Rev. D19 (1979) 221.

12. UA1 Collaboration, G. Arnison et al., Phys. Lett. 139B (1984) 115.

13. UA2 Collaboration, P. Bagnaia et al., Phys. Lett. 139B (1984) 105.

14. P. Aurenche and R. Kinnunnen, LAPP-TH-108 (1984);
A. Ballestrero and G. Passarino, Torino Univ. preprint IFTT-435 (1984).

15. R. K. Ellis, G. Martinelli and R. Petronzio, Nucl. Phys. B211 (1983) 106.

16. G. T. Bodwin, S. J. Brodsky and G. P. Lepage, Phys. Rev. Lett. 47 (1981) 1799.

17. W. W. Lindsay, D. A. Ross and C. T. Sachrajda, Nucl. Phys. B214 (1983) 61.

18. D. W. Duke and J. F. Owens, Phys. Rev. D30 (1984) 49.

19. M. Gluck, E. Hoffmann and E. Reya, Z. Phys. C13 (1982) 119.

20. E. Eichten, I. Hinchliffe, K. Lane and C. Quigg, Rev. Mod. Phys. 56 (1984).

21. For a review, see G. Altarelli, Phys. Rep. 81 (1982) 1.

22. G. Parisi, Phys. Lett. 90B (1980) 295;
G. Curci and M. Greco, Phys. Lett. 92B (1980) 175.

23. J. C. Collins, D. E. Soper and G. Sterman, CERN-TH 3923 (1984).

24. J. Kubar-Andre, M. Le Bellac, J. L. Meunier and G. Plaut, Nucl. Phys. B175 (1980) 251.

25. G. Altarelli and G. Parisi, Nucl. Phys. B126 (1977) 298.

26. L. V. Gribov, E. M. Levin, M. G. Ryskin, Nucl. Phys. B188 (1981) 555; Phys. Rep. 100 (1983) 1. J. C. Collins, Proceedings of the 1984 Snowmass Workshop on Supercollider Physics.

27. A. Bassetto, M. Ciafaloni, G. Marchesini; Phys. Rep. 100 (1983) 201.

28. A. Bassetto, M. Ciafaloni and G. Marchesini, Nucl. Phys. B163 (1980) 477.
A. H. Mueller, Phys. Lett. 104B (1981) 161;
A. Bassetto, M. Ciafaloni, G. Marchesini and A. H. Mueller, Nucl. Phys. B207 (1982) 189.

29. A. H. Mueller, Nucl. Phys. B213 (1983) 85.

30. G. Curci, W. Furmanski, R. Petronzio, Nucl. Phys. B175 (1980) 27.
E. G. Floratos, R. Lacaze and C. Kounnas, Phys. Lett. 98B (1981) 89.

31. T. Jaroszewicz, Phys. Lett. 116B (1982) 291.

32. T. Kinoshita, J. Math. Phys. 3 (1962) 650;
T. Kinoshita, A. Sirlin, Phys. Rev. 113 (1959) 1652;
T. D. Lee and M. Nauenberg, Phys. Rev. 133 (1964) 1549.

33. E. L. Berger and D. E. Soper, CERN-TH 3850 (1983).

TABLE CAPTIONS

1. Theoretical results for the W and Z total cross-sections in $p\bar{p}$ interactions at various energies. Estimates of the theoretical error are also given.

2. The percentage probability $\pi(q^0_T)$ as a funtcion of q^0_T, for W and Z bosons at $\sqrt{S}$ = 540, 630 GeV.

3. The percentage probability $\pi^W(q^0_T)$ including the order (α^2_s) $q\bar{q}$ correction at $\sqrt{s}$ = 540 GeV. with $\Lambda_{\overline{MS}}$ =0.1 ~ 0.3 GeV.

4. The percentage probability $\pi^W(q^0_T)$ at $\sqrt{S}$=1.6 and 10 TeV as a function of q^0_T.

5. The W production cross section $x(y,q_T) = 1/\sigma\ d\sigma/dq_T dy \cdot 10^3$ GeV^{-1} in $p\bar{p}$ collisions at $\sqrt{S}$ = 0.63 TeV.

Table 1

$\sqrt{S}$(TeV)	$\sigma^{W^+ + W^-}$ (M_W=83 GeV) (nb)	σ^{Z^0} (M_{Z^0}=94 GeV) (nb)
0.54	$4.2^{+1.3}_{-0.6}$	$1.3^{+0.4}_{-0.2}$
0.63	$5.3^{+1.6}_{-0.9}$	$1.6^{+0.5}_{-0.3}$
1.6	$16.0^{+4.0}_{-2.5}$	$4.9^{+1.2}_{-0.8}$
2.	$20.^{+6.}_{-4.}$	$6.2^{+1.9}_{-1.2}$
10.	$75.^{+35.}_{-25.}$	$27.^{+12.}_{-9.}$
20.	$130.^{+70.}_{-55.}$	$46.^{+24.}_{-20.}$
40.	$190.\pm100.$	$70.\pm30.$

Table 3

q_T^0	$\pi^W(q_T^0)$%
25	3.4 ±0.4
30	2.0 ±0.2
40	0.8 ±0.1
50	0.4 ±0.05
60	0.16±0.02

Table 2

q_T^o	$\pi^W(q_T^o)\%$	$\pi^Z(q_T^o)\%$	
25	4.4 ±2.0	5.1 ±2.5	
30	2.7 ±1.1	3.2 ±1.3	
35	1.7 ±0.7	2.0 ±0.8	
40	1.1 ±0.4	1.4 ±0.5	$\sqrt{S}$ = 540 GeV.
45	0.7 ±0.3	0.9 ±0.3	
50	0.5 ±0.1	0.6 ±0.2	
55	0.30±0.07	0.40±0.10	
60	0.20±0.05	0.25±0.08	

q_T^o	$\pi^W(q_T^o)\%$	$\pi^Z(q_T^o)\%$	
25	5.4 ±2.3	6.1± 2.8	
30	3.5 ±1.3	4.0 ±1.6	
35	2.3 ±0.8	2.6 ±1.0	
40	1.5 ±0.5	1.8 ±0.6	$\sqrt{S}$ = 630 GeV
45	1.0 ±0.3	1.2 ±0.4	
50	0.7 ±0.2	0.9 ±0.2	
55	0.50±0.15	0.60±0.15	
60	0.30±0.09	0.40±0.12	

Table 4

q_T	$\pi^W(q_T^o)$% at $\sqrt{S}$ = 1.6 TeV	$\pi^W(q_T^o)$% at $\sqrt{S}$ = 10 TeV
30	8.9	26.0
40	5.3	16.9
50	3.3	11.7
60	2.1	8.3
70	1.4	6.0
80	0.9	4.5
90	0.6	3.4
100	-	2.6
110	-	2.1
120	-	1.7
130	-	1.3
140	-	1.1
150	-	0.9
160	-	0.7
170	-	0.6
180	-	0.5

Table 5

q_T GeV	$x(0,q_T)$	$x(0,5,q_T)$	$x(0.75,q_T)$	$x(1.0,q_T)$	$x(1.25,q_T)$	$x(1.50,q_T)$	$x(1.75,q_T)$
1	43.8	39.6	34.1	26.3	16.7	7.2	1.2
2	61.8	55.6	47.7	36.5	23.0	9.9	1.6
3	59.9	53.6	45.6	34.5	21.4	9.0	1.4
4	51.4	45.6	38.4	28.6	17.4	7.1	1.1
5	42.5	37.3	31.0	22.7	13.5	5.3	<1
6	34.6	30.0	24.7	17.7	10.3	3.9	-
7	28.1	24.2	19.6	13.8	7.8	2.8	-
8	23.2	19.9	16.0	11.1	6.2	2.1	-
9	19.6	16.7	13.4	9.3	5.1	1.7	-
10	16.7	14.2	11.3	7.8	4.3	1.5	-
11	14.1	12.0	9.6	6.6	3.6	1.2	-
12	11.9	10.1	8.0	5.5	3.0	1.0	-
13	10.5	8.8	7.0	4.8	2.5	<1.0	-
14	9.4	7.8	6.2	4.2	2.2	-	-
15	8.2	6.8	5.3	3.6	1.8	-	-
16	7.3	5.9	4.6	3.0	1.5	-	-
17	6.4	5.1	4.0	2.5	1.2	-	-
18	5.4	4.3	3.2	2.0	<1.0	-	-
19	4.7	3.8	2.8	1.7	-	-	-
20	4.3	3.4	2.6	1.6	-	-	-
21	3.8	3.1	2.3	1.4	-	-	-
22	3.2	2.7	2.0	1.3	-	-	-
23	2.7	2.2	1.6	<1.0	-	-	-
24	2.6	2.1	1.5	-	-	-	-
25	2.5	2.0	1.4	-	-	-	-
26	2.3	1.7	1.3	-	-	-	-
27	2.1	1.6	1.1	-	-	-	-
28	2.0	1.4	1.0	-	-	-	-
29	1.8	1.3	<1.0	-	-	-	-
30	1.6	1.2	-	-	-	-	-

FIGURE CAPTIONS

Fig. 1. The parton distribution functions f used in this paper as a function of x at Q = 83 GeV. g, $\bar{u}$ and $u_v = u-\bar{u}$ refer to the gluon, the anti-quark and the valence up quark distributions. The solid lines are the distributions of ref. 18 (DO1, Λ = 0.2 GeV), the dashed lines are the distributions of ref. 19 (GHR, Λ = 0.4 GeV), and the dotted lines are the distributions of ref. 20 (EHLQ1, Λ = 0.2 GeV).

Fig. 2. The combinations of products of parton distributions relevant for W production in proton-antiproton collisions; $H^W = (u\bar{d} + c\bar{s})\cos^2\theta_C + (u\bar{s} + c\bar{d})\sin^2\theta_C$, $K^W = (u + c + \bar{d} + \bar{s})g$ (see Eq. (66-68) of ref. 1). Solid line: DO1, Λ = 0.2 GeV, ref. 18, Dashed line: GHR, Λ = 0.4 GeV, ref. 19. Dotted line: EHLQ1, Λ = 0.2 GeV, ref. 20.

Fig. 3. The ratio $R = (d\sigma/dq_T dy)/(d\sigma/dy)$ at y = 0 as a function of q_T. The curves are plotted for $\sqrt{S}$ = 0.63, 1.6, 10 and 20 TeV. Parton distributions: DO1, Λ = 0.2.

Fig. 4. The dimensionless quantity $\Sigma = q_T\,(d\sigma/dq_T dy)/(d\sigma/dy)$ at y = 0 as a function of $x_T = 2q_T/\sqrt{S}$, for different values of $\sqrt{S}$ but with $\sqrt{\tau}$ fixed at the value $\sqrt{\tau}$ = 0.13. Parton distributions: DO1, Λ = 0.2, ref. 18.

Fig. 5. Total cross-sections for the production of $W^+ + W^-$ (M_W = 83) and hypothetical W's of heavier mass vs. centre of mass energy. The solid line is for proton-antiproton collisions and the dashed line for proton-proton collisions. (Distributions DO1, Λ = 0.2 GeV).

Fig. 6. $S\sigma^{W^+ + W^-}$ plotted against $1/\sqrt{\tau}$ for various values of the centre of mass energy ranging between 0.54 and 20 TeV. The parton distributions of ref. 19 were used (GHR, Λ = 0.4 GeV).

Fig. 7 The distribution $[(d\sigma/dy)/\sigma]$ vs. rapidity y at various values of $\sqrt{S}$ for M_W = 83. The black squares near to the curve at $\sqrt{S}$ = 0.63 TeV represent the results obtained at $\sqrt{S}$ = 10 TeV for a vector boson mass which gives the same value of τ as the solid curve. (i.e. M = 1320 GeV). Parton distributions: DO1, Λ = 0.2 GeV, ref. 18.

Fig. 8. Comparison of the resummed expression for $(d\sigma/dq_T dy)\big|_{y=0}$ (solid line) with the first order perturbative expression (dashed line) at $\sqrt{S}$ = 0.63 TeV using the parton distributions of ref. 19 (GHR, Λ = 0.4 GeV).

Fig. 9. Same as Fig. 8 with $\sqrt{S}$ = 10 TeV.

Fig. 10. The average value of q_T in $p\bar{p}$ collisions as a function of $\sqrt{S}$ for three values of τ (the couplings are fixed as for ordinary W production but the mass Q is changed). The solid line indicates the average transverse momentum for the production of the W. Distributions: DO1, Λ = 0.2, ref. 18.

Fig. 11. The same as in Fig. 10 but for the root mean square of the transverse momentum.

Fig. 12. The same as in Fig. 10 but for proton-proton rather than for proton-antiproton collisions.

Fig. 13. The ratio $R = (d\sigma/dq_T dy)/(d\sigma/dy)$ at $\sqrt{S}$ = 630 GeV and different values of the rapidity y. Distributions: DO1, Λ = 0.2 GeV, ref. 18.

Fig. 14. Normalised rapidity distribution for W production at $\sqrt{S}$ = 630 GeV. Distributions: DO1, Λ = 0.2 GeV, ref. 18.

Fig. 15. The lepton pair production cross-section at $\sqrt{S}$ = 540 GeV as a function of the pair mass Q. Only the virtual photon contribution is included in this plot. Parton distributions: DO1, Λ = 0.2 GeV, ref. 18.

Fig. 16. Normalised rapidity distribution $F(y) = (d\sigma/dQ^2 dy)/(d\sigma/dQ^2)$ for lepton pair production at $\sqrt{S}$ = 540 GeV for different values of the lepton pair mass, computed as described in Fig. 15.

Fig. 17. Normalised q_T distribution $R = (d\sigma/dq_T dy)/(d\sigma/dy)$ at y=0 for lepton pair production at $\sqrt{S}$ = 540 GeV for different values of the lepton pair mass, computed as in Fig. 15.

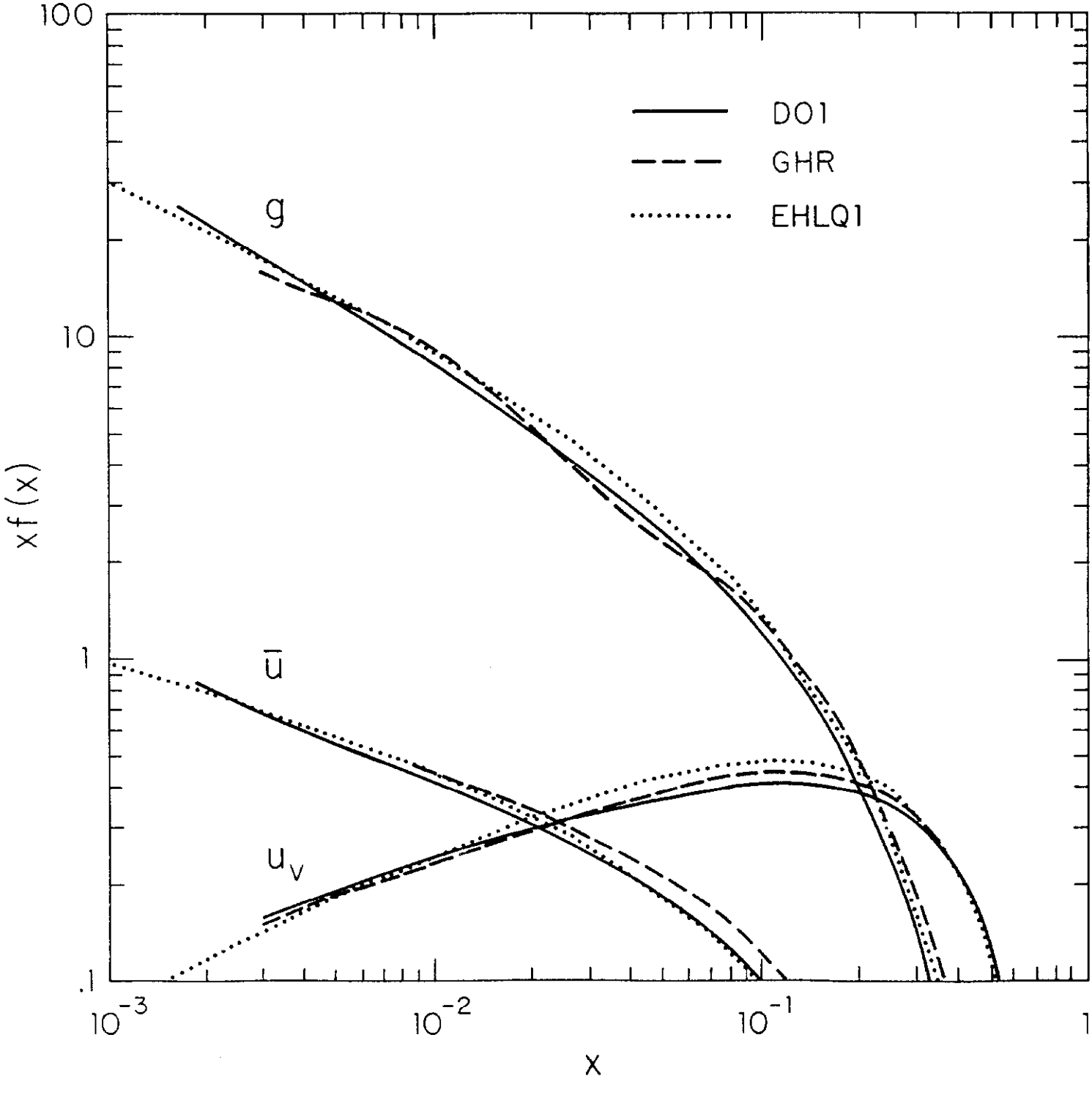

Figure 1

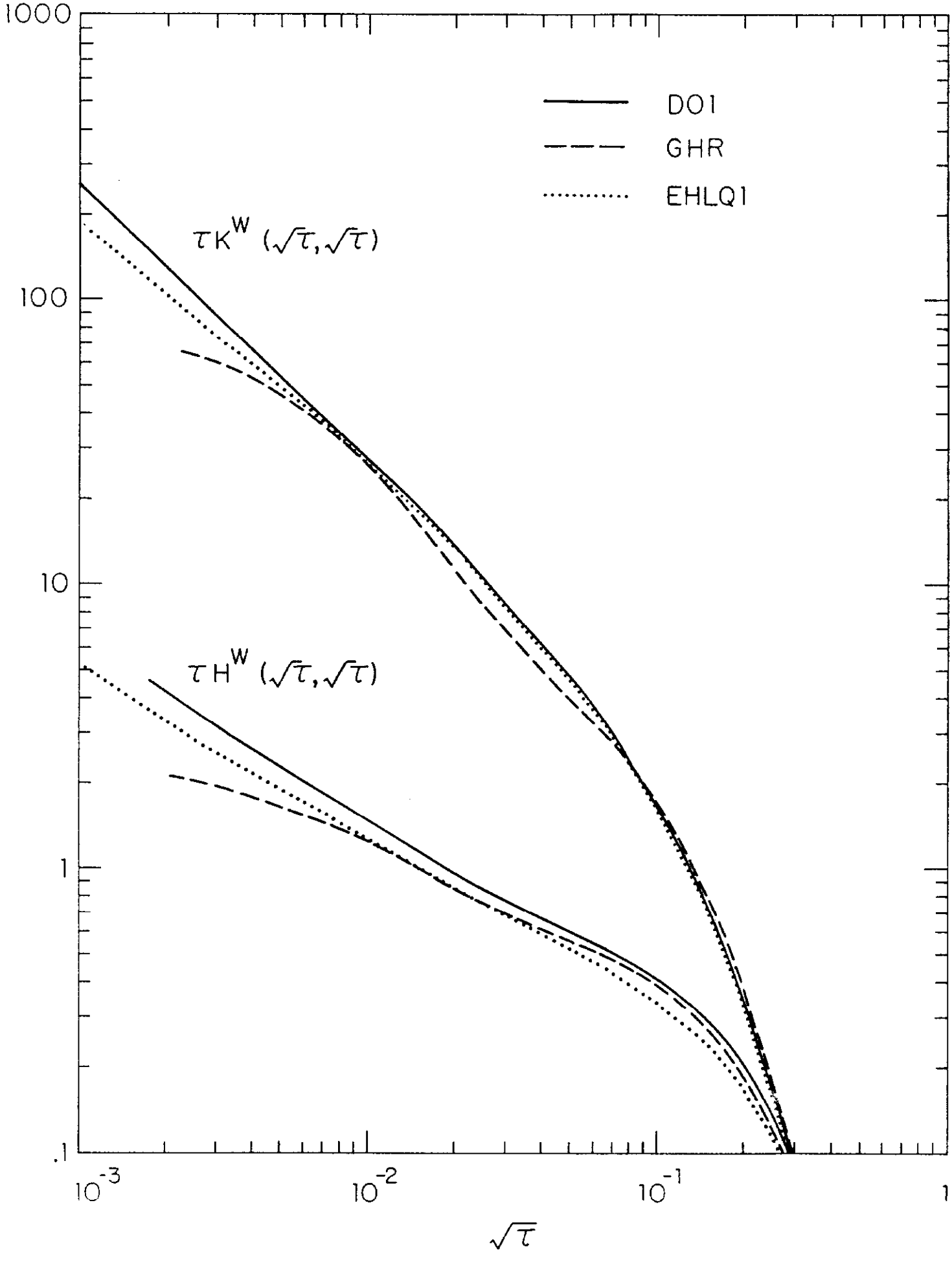
1000
100
10
1
.1
DO1
GHR
EHLQ1
$\tau K^W(\sqrt{\tau},\sqrt{\tau})$
$\tau H^W(\sqrt{\tau},\sqrt{\tau})$
10^{-3}
10^{-2}
10^{-1}
1
$\sqrt{\tau}$

Figure 2